
Optimal Control of Machine Tool Manipulators

Bahne Christiansen¹, Helmut Maurer¹ and Oliver Zirn²

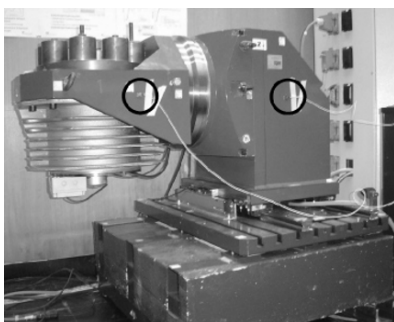
¹ Institut für Numerische Mathematik und Angewandte Mathematik,
Westfälische Wilhelms-Universität Münster,
christiansen@wwu.de, maurer@math.uni-muenster.de

² Institut für Prozess- und Produktionsleittechnik
Technische Universität Clausthal,
zirn@ipp.tu-clausthal.de

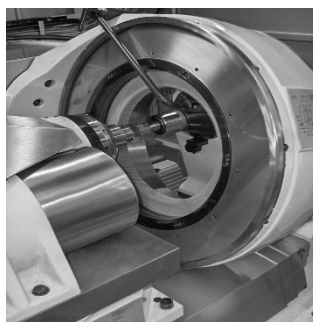
Summary. Based on the dynamical models for machine tool manipulators in Zirn [11, 12], we compare state-of-the-art feedback controls with optimal controls that either minimize the transfer time or damp vibrations of the system. The damping performance can be improved substantially by imposing state constraints on some of the state variables. Optimal control results give hints for suitable jerk limitations in the setpoint generator of numerical control systems for machine tools.

1 Introduction

Fig. 1 shows two typical machine tool manipulators. Both are representative for the dynamical model presented in the following section.



(a) Milling Machine Tool Workpiece Manipulator



(b) Honing Machine Tool Manipulator

Fig. 1. Typical Machine Tool Manipulators.

Fig. 1(a) displays a manipulator on the workpiece side of a 5-axis milling machine with the translatory X-axis driven by a linear motor and two rotary axes. The performance of the linear X-axis is limited significantly by the flexible mechanical structure. Although the voice-coil-motor servo axis that we discussed in [2] also carries a flexible load, Coulombic friction represents the dominating influence on the dynamic axis performance of that example. For the machine tool axis discussed here, the guide friction is comparably small and can be compensated with moderate effort in the axis controller. Fig. 1(b) shows a honing machine tool for the fine finishing of gear wheels. This manipulator has two translatory Z-axes, one for the honing wheel, which is the mid abrasive honing stone, and a second one for the gear wheel.

2 Dynamic control model of a machine tool manipulator

The dynamic process of a machine tool manipulator is considered in the time interval $t \in [0, t_f]$ with t measured in seconds; the final time t_f is either fixed or free. The state variables are as follows: the base position $x_b(t)$, the slider position $x_s(t)$, the slider rotary position $\varphi(t)$, the corresponding velocities $v_b(t)$, $v_s(t)$ and $v_\varphi(t)$ and the X-axis linear motor force $F(t)$. The input variable (control) of the motor is the setpoint motor force $F_{\text{set}}(t)$. The dynamics is given by the following system of linear differential equations, where as usual the dot denotes the time derivative. System parameters are listed in Tab. 1.

$$\begin{aligned} \dot{x}_b(t) &= v_b(t), & \dot{v}_b(t) &= -\frac{1}{m_b} (k_b x_b(t) + d_b v_b(t) + F(t)), \\ \dot{x}_s(t) &= v_s(t), & \dot{v}_s(t) &= \frac{1}{m_s} F(t), \\ \dot{\varphi}(t) &= v_\varphi(t), & \dot{v}_\varphi(t) &= \frac{1}{J} (rF(t) - k\varphi(t) - d v_\varphi(t)), \\ \dot{F}(t) &= \frac{1}{T} (F_{\text{set}}(t) - F(t)). \end{aligned} \tag{1}$$

The control constraint is given by

$$-F_{\text{max}} \leq F_{\text{set}}(t) \leq F_{\text{max}}, \quad 0 \leq t \leq t_f, \tag{2}$$

Base mass	$m_b = 450 \text{ kg}$
Slider mass	$m_s = 750 \text{ kg}$
Slider inertia	$J = 40 \text{ kg m}^2$
Slider centre of gravity excentricity - guides	$r = 0.25 \text{ m}$
Slider centre of gravity excentricity - TCP	$h = 0.21 \text{ m}$
Stiffness of the base anchorage	$k_b = 4.441 \cdot 10^7 \text{ N/m}$
Damping constant of the base anchorage	$d_b = 8500 \text{ Ns/m}$
Stiffness of the fictive rotary joint torsion spring	$k = 8.2 \cdot 10^6 \text{ Nm/rad}$
Damping constant of the fictive rotary joint torsion spring	$d = 1800 \text{ Nms/rad}$
Current control loop time constant	$T = 2.5 \text{ ms}$
Maximum input force	$ F_{\text{max}} \leq 4 \text{ kN}$

Table 1. List of system parameters

where $F_{\max} \leq 4\text{ kN}$ holds for mechanical reasons. The initial and terminal conditions for the state vector $x = (x_b, x_s, \varphi, v_b, v_s, v_\varphi, F)^* \in \mathbb{R}^7$ are given by

$$x(0) = (0, 0, 0, 0, 0, 0, 0)^*, \quad x(t_f) = (0, \text{undef.}, 0, 0, 0, 0.1, 0, 0)^*. \quad (3)$$

3 Feedback control performance

The state-of-the-art feedback control for CNC machine tools is shown as a block diagram in Fig. 2.

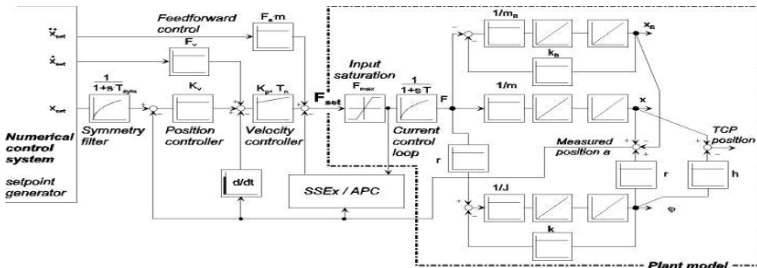
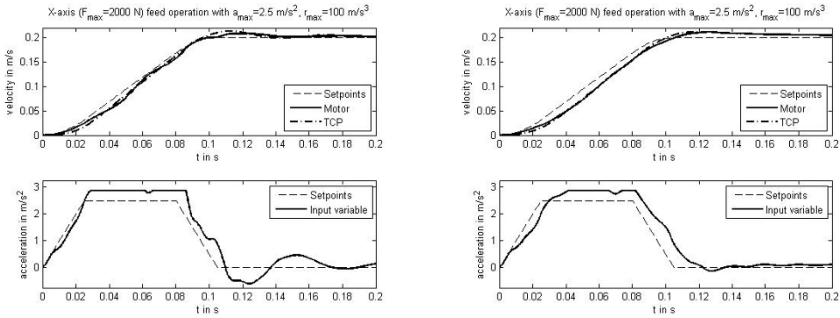


Fig. 2. Block diagramm for feedback control

The velocity-, acceleration- and jerk-limited setpoints generated by the numerical control system are feedback controlled by a cascade controller with velocity and position control loop and a state space control extension to improve the active structural vibration damping for the dominant mode. Compared to robots, where TCP vibrations caused by rough setpoints and flexible structure can hardly be identified by the motor measurement systems and are eliminated by short waiting times after positioning operations, the requirements for machine tool manipulators are much more challenging. Due to the milling or grinding process, all TCP vibrations are visible directly on the workpiece. So it is mandatory that the input variables never excite remarkable structural vibrations at all. Machine tools measure their drive states not only at the motor but also quite near to the TCP, so it is possible to damp structural vibrations by the feedback servo controller. But in practice, the achievable damping is not sufficient and vibration-free control values remain an important future issue for machine tools.

The plant model is the block diagram representation of the differential equations discussed in Sec. 2. In Fig. 3(a), the typical setpoints F_{set} that result from such a control concept are shown for an exemplary acceleration operation of the axis: The optimum productivity in combination with suitable damping performance is achieved for significant jerk control, i.e. the maximum acceleration has to be achieved by smooth setpoints. Also with state space control, the suitable setpoints have a typical trapezoidal shape, cf. Fig. 3(b). The practical experience with many machine tool axis control applications



(a) Pure cascade controlled system (b) Axis with state space control extensions

Fig. 3. State-of-the-art feedback control for CNC machine tools

shows that the possible jerk depends on the eigenfrequency of the dominating mode, but no commissioning rules have been derived up to now.

Fig. 3(b) indicates two deficiencies of feedback controls: (i) the terminal position is not attained precisely leading to a terminal overshooting, (ii) the transfer time is much larger than the minimal transfer time computed via optimal control methods in the following sections.

4 Optimal control models of machine tool manipulators

The dynamic equation (1) can be written in compact linear form as

$$\dot{x} = f(x, F_{\text{set}}) = Ax + BF_{\text{set}} \tag{4}$$

with a matrix $A \in \mathbb{R}^{7 \times 7}$ and a column vector $B \in \mathbb{R}^{7 \times 1}$. Since the process duration is an important criterion for the efficient usage of machine tool manipulators, we first consider the control problem of minimizing the final time t_f subject to the conditions (1)–(3). It turns out that some of the time-optimal state trajectories are highly oscillatory. Damping of oscillations can be achieved by an alternative cost functional that is quadratic in control and state variables,

$$\text{minimize } \int_0^{t_f} F_{\text{set}}^2 + c_1 x_b^2 + c_2 \varphi^2 + c_3 v_b^2 + c_4 v_\varphi^2 dt \quad (\text{fixed } t_f > 0), \tag{5}$$

where $c_1, c_2, c_3, c_4 > 0$ are appropriate constants. Of course, the fixed final time t_f in the cost functional (5) must be larger than the minimal time t_f^{min} . Note that we keep the control constraint (2). Another approach to avoid larger oscillations consists in imposing state constraints of the form

$$-c_\varphi \leq v_\varphi(t) \leq c_\varphi, \quad t \in [0, t_f], \tag{6}$$

with a prescribed constant $c_\varphi > 0$, cf. Sec. 5.2.

5 Time-optimal control

Pontryagin’s Minimum Principle involves the adjoint variable (row vector) $\lambda = (\lambda_{x_b}, \lambda_{x_s}, \lambda_\varphi, \lambda_{v_b}, \lambda_{v_s}, \lambda_{v_\varphi}, \lambda_F) \in \mathbb{R}^7$ and the Hamiltonian function

$$H(x, \lambda, F_{\text{set}}) = 1 + \lambda(Ax + BF_{\text{set}}). \tag{7}$$

The adjoint λ satisfies the linear adjoint equation $\dot{\lambda} = -\lambda A$,

$$\begin{aligned} \dot{\lambda}_{x_b} &= \frac{k_b}{m_b} \lambda_{v_b}, & \dot{\lambda}_{x_s} &= 0, & \dot{\lambda}_\varphi &= \frac{k}{J} \lambda_{v_\varphi}, & \dot{\lambda}_{v_b} &= -\lambda_{x_b} + \frac{d_b}{m_b} \lambda_{v_b}, \\ \dot{\lambda}_{v_s} &= -\lambda_{x_s}, & \dot{\lambda}_{v_\varphi} &= -\lambda_\varphi + \frac{d}{J} \lambda_{v_\varphi}, & \dot{\lambda}_F &= \frac{1}{m_b} \lambda_{v_b} - \frac{1}{m_s} \lambda_{v_s} - \frac{r}{J} \lambda_{v_\varphi} + \frac{1}{T} \lambda_F. \end{aligned} \tag{8}$$

We have $\lambda_{x_s}(t_f) = 0$, since the terminal state $x_s(t_f)$ is free. Then the adjoint equations (8) imply $\lambda_{x_s}(t) = 0$ and $\lambda_{v_s}(t) = \text{const}$ for all $0 \leq t \leq t_f$. The optimal control $F_{\text{set}}(t)$ minimizes the Hamiltonian function on the control set $-F_{\text{max}} \leq F_{\text{set}}(t) \leq F_{\text{max}}$. This gives the control law

$$F_{\text{set}}(t) = -\text{sign}(\lambda_F(t))F_{\text{max}}. \tag{9}$$

The linear system (4) is completely controllable, since the 7×7 Kalman matrix

$$C = (B, AB, A^2B, A^3B, A^4B, A^5B, A^6B) \tag{10}$$

has maximal rank 7. Hence, the time-optimal control $F_{\text{set}}(t)$ is of bang–bang type; cf. [5].

The optimal control problem is solved by a discretization approach using Euler’s method or a higher order Runge–Kutta integration method. The resulting large-scale optimization problem is implemented via the modeling language AMPL [3] and is solved by the interior point optimization solver IPOPT due to Wächter et al. [10]. Alternatively, we use the optimal control package NUDOCSS developed by Büskens [1]. Computations with $N = 10000$ grid points show that for all values of $F_{\text{max}} > 0$ the control has the following structure with 5 switching times $0 =: t_0 < t_1 < t_2 < t_3 < t_4 < t_5 < t_f$ and the free final time $t_6 := t_f$:

$$F_{\text{set}}(t) = \left\{ \begin{array}{l} F_{\text{max}} \text{ for } t_0 \leq t < t_1 \\ -F_{\text{max}} \text{ for } t_1 \leq t < t_2 \\ F_{\text{max}} \text{ for } t_2 \leq t < t_3 \\ -F_{\text{max}} \text{ for } t_3 \leq t < t_4 \\ F_{\text{max}} \text{ for } t_4 \leq t < t_5 \\ -F_{\text{max}} \text{ for } t_5 \leq t \leq t_6 \end{array} \right\}. \tag{11}$$

This control structure is not surprising, since one intuitively expects that six degrees of freedom, namely the six variables $t_i, i = 1, \dots, 6$, would suffice to satisfy the six terminal conditions in (3). The discretization and optimization

approach provides switching times that are correct up to 3 – 4 decimals. The arc-parametrization method in [7] then allows us to compute the switching times with higher precision which simultaneously provides a test of optimality [8, 9]. In this method, the *arclengths* of the bang–bang arcs defined by $\xi_j = t_j - t_{j-1}$, ($j = 1, \dots, 6$), $t_0 := 0$, $t_6 := t_f$ are optimized directly using again the code NUDOCCCS [1].

5.1 Numerical results

Fig. 4 displays the optimal solution for the control constraint $F_{\max} = 2 \text{ kN}$. The switching times and final time are computed as

$$\begin{aligned} t_1 &= 0.009337, & t_2 &= 0.009668, & t_3 &= 0.036552, \\ t_4 &= 0.037653, & t_5 &= 0.041942, & t_f &= 0.043505. \end{aligned} \tag{12}$$

The initial value of the adjoint variable $\lambda(t) \in \mathbb{R}^7$ satisfying the adjoint equation (8) is given by

$$\begin{aligned} \lambda(0) &= (-11.87902, 0.00000, 14.75425, 0.05508, \\ &\quad -0.23018, 0.01149, -1.2503 \cdot 10^{-6}). \end{aligned}$$

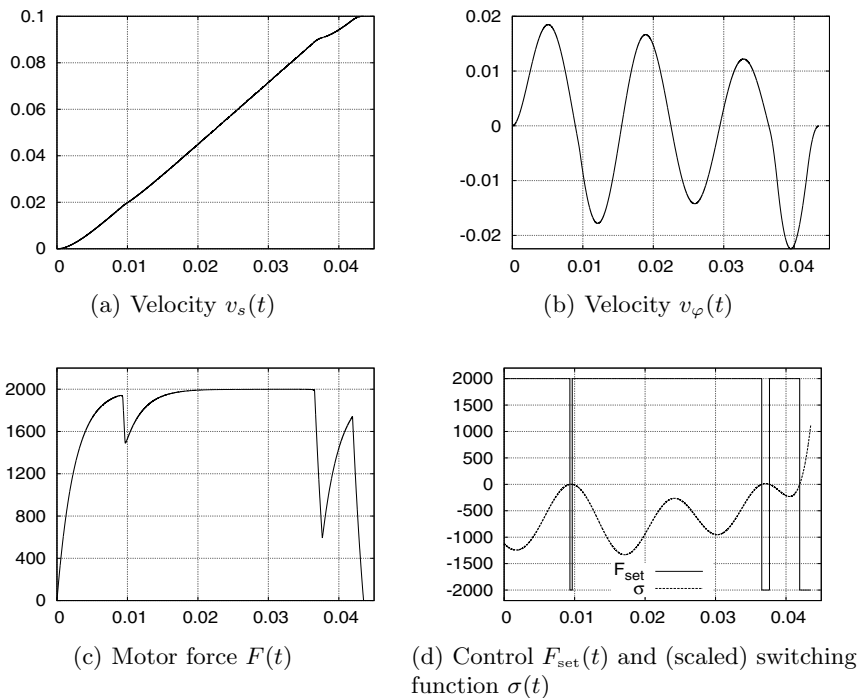


Fig. 4. Time-optimal solution for control bound $F_{\max} = 2 \text{ kN}$

With these values the reader may verify that the switching function $\sigma(t) := H_{F_{\text{set}}}(t) = \lambda_F(t)/T$ obeys the control law (9) with high accuracy; cf. Fig. 4(d). The local optimality of this trajectory follows from the fact that the 6×6 Jacobian matrix of the terminal conditions computed with respect to the switching times and final time has full rank. Hence, first order sufficient conditions are satisfied for this time-optimal problem; cf. [8, 9].

5.2 State constraints

Higher values of the control bound F_{max} lead to higher vibrations in the machine tool system. Hence, it is reasonable to impose constraints on the oscillating state variables. We restrict the discussion to vibrations of the slider tower φ and consider the state constraint $|v_\varphi(t)| \leq c_\varphi$ for the velocity. Following the notations in [4, 6], this can be written as two inequalities

$$S_1(x) := v_\varphi(t) - c_\varphi \leq 0, \quad S_2(x) := -c_\varphi - v_\varphi(t) \leq 0. \tag{13}$$

Computations show that by imposing these constraints we can also achieve a significant reduction of the deviation $\|\varphi(t)\|_\infty$. The reader is referred to [4, 6] for the discussion of necessary conditions for state-constrained optimal control problems. It suffices to analyze the component S_1 . The constraint has order 2 since the control variable F_{set} appears for the first time in the second time derivative of S_1 ,

$$\frac{d^2}{dt^2} S_1(x) = \frac{d^2 - k}{J} v_\varphi + \frac{dk}{J} \varphi - \left(\frac{r}{JT} + \frac{rd}{J^2} \right) F + \frac{r}{JT} F_{\text{set}}.$$

A *boundary arc* $[t_{\text{en}}, t_{\text{ex}}]$ for the constraint $S_1(x) \leq 0$ is characterized by the equation $S_1(x(t)) = 0$ for $t_{\text{en}} \leq t \leq t_{\text{ex}}$ (t_{en} : entry-time, t_{ex} : exit-time). Along a boundary arc the equation $d^2 S_1(t)/dt^2 = 0$ holds, from which we obtain the following feedback expression for the *boundary control*:

$$F_{\text{set}}^{(b)}(x) = \frac{T(k - d^2)}{r} v_\varphi - \frac{Tdk}{r} \varphi + \left(1 + \frac{Td}{J} \right) F.$$

The augmented Hamiltonian \tilde{H} is obtained from the Hamiltonian H by adjoining the state constraint with a multiplier $\mu_1 \in \mathbb{R}$,

$$\tilde{H}(x, F_{\text{set}}, \lambda, \mu_1) = 1 + \lambda(Ax + BF_{\text{set}}) + \mu_1(v_\varphi - c_\varphi).$$

Assuming as in [4, 6] that the boundary control $F_{\text{set}}^{(b)}(x)$ lies in the interior of the control set, it follows from the minimum principle that the switching function vanishes along a boundary arc:

$$\frac{1}{T} \lambda_I(t) = \tilde{H}_U(t) = 0 \quad \text{for } t_{\text{en}} \leq t \leq t_{\text{ex}}. \tag{14}$$

From the equation $d^2 \lambda_F/dt^2 = 0$, $t_{\text{en}} \leq t \leq t_{\text{ex}}$, we obtain the relation

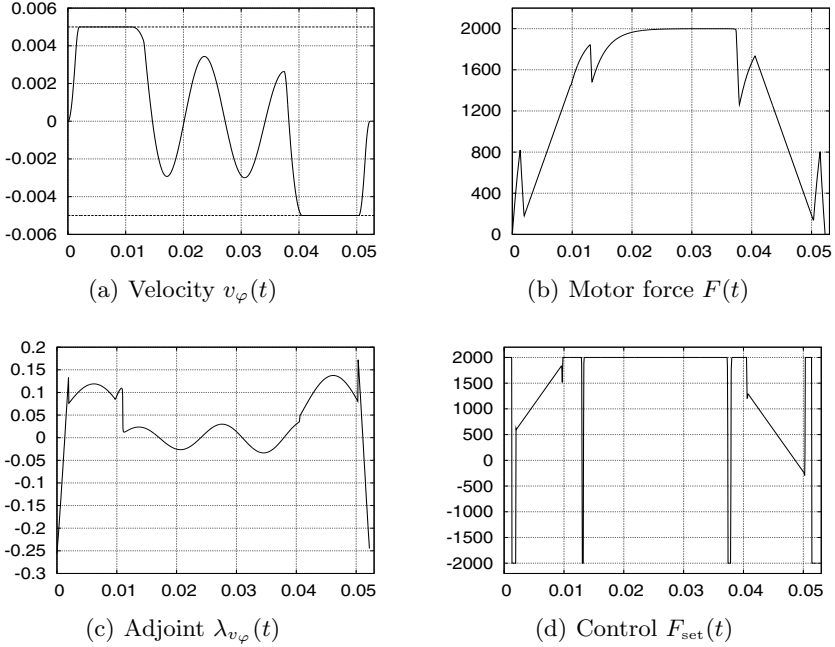


Fig. 5. Time-optimal solution for control bound $F_{\max} = 2$ kN and state constraint $|v_\varphi(t)| \leq c_\varphi = 0.005$

$$\mu_1 = \mu_1(\lambda) = \frac{J}{rm_b} \lambda_{x_b} - \lambda_\varphi - \frac{Jd_b}{rm_b^2} \lambda_{v_b}. \tag{15}$$

The adjoint variable $\lambda_{v_\varphi}(t)$ may have jumps at the entry and exit time $\tau \in \{t_{\text{en}}, t_{\text{ex}}\}$; cf. [4, 6]. Fig. 5 displays the optimal solution for the rather rigorous bound $c_\varphi = 0.005$. The optimal control has one boundary arc with $v_\varphi(t) = c_\varphi$, one boundary arc with $v_\varphi(t) = -c_\varphi$ and altogether nine interior bang–bang arcs, two of which are located before the first interior arc, five between the interior arcs and two after the last boundary arc. The final time $t_f = 0.0522$ is about 23% higher than in the unconstrained case (12).

6 Damping-optimal control

We consider the “damping-optimal” cost functional (5) of minimizing

$$\int_0^{t_f} (F_{\text{set}}^2 + c_1 x_B^2 + c_2 \varphi^2 + c_3 v_B^2 + c_4 v_\varphi^2) dt,$$

with a fixed final time $t_f > t_f^{\min}$, where t_f^{\min} is the minimal time computed in Sec. 5.1. The weights $c_i, i = 1, \dots, 4$, are equilibrated in such a way that

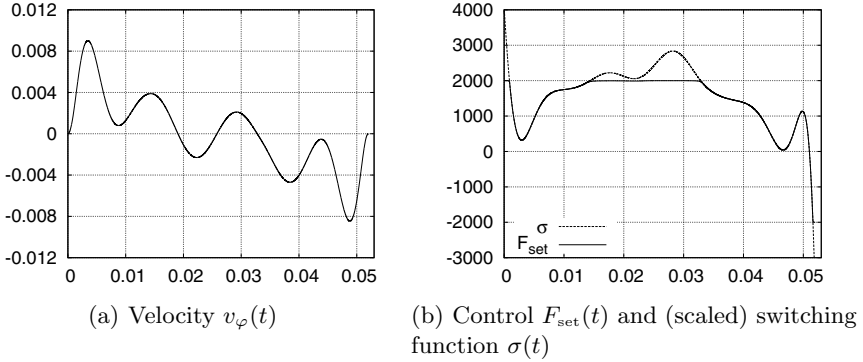


Fig. 6. Damping-optimal solution for control bound $F_{\text{max}} = 2\text{kN}$, final time $t_f = 0.0522$ and weights (17).

all terms in the quadratic cost functional (5) have the same magnitude. The Hamiltonian

$$H(x(t), \lambda(t), F_{\text{set}}) = F_{\text{set}}^2 + c_1 x_B^2(t) + c_2 \varphi^2(t) + c_3 v_B^2(t) + c_4 v_\varphi^2(t) + \lambda(t)(Ax(t) + BF_{\text{set}})$$

is regular and admits a unique minimizer

$$F_{\text{set}}(t) = \text{Proj}_{[-F_{\text{max}}, F_{\text{max}}]} (-\lambda_F(t) / 2T), \tag{16}$$

where Proj denotes the projection onto the control set. Since the convexity conditions of the second order sufficient conditions (SSC) in [4] are satisfied, the optimality of the presented solution is guaranteed. The adjoint variables satisfy the adjoint equations $\dot{\lambda} = -2Dx - \lambda A$ with the diagonal matrix $D = \text{diag}(c_1, 0, c_2, c_3, 0, c_4)$. In particular, the control law (16) shows that any optimal control is *continuous*. Fig. 6 displays the optimal solution for the fixed final time $t_f = 0.0522$ that is the minimal time under the state constraint $|v_\varphi(t)| \leq c_\varphi = 0.005$. The weights are given by

$$c_1 = 1.8858 \cdot 10^{15}, c_2 = 1.0961 \cdot 10^{15}, c_3 = 8.6070 \cdot 10^{10}, c_4 = 2.8505 \cdot 10^{10}. \tag{17}$$

Fig. 6(b) clearly confirms the control law (16). For this control we get $\|\varphi(t)\|_\infty = 0.008916$. Though this value is notably higher than the prescribed bound $\|\varphi(t)\|_\infty = 0.005$ for the time-optimal solution, it is significantly smaller than the value $\|\varphi(t)\|_\infty = 0.022444$ obtained for the unconstrained time-optimal control.

7 Conclusion

In this paper, we have studied time-optimal and damping-optimal controls for typical machine tool manipulators. Time-optimal controls are bang-bang, for

which optimality can be established by second order conditions [7, 8, 9]. The damping performance of time-optimal solutions can be significantly improved by imposing suitable state constraints. Damping-optimal controls are found as solutions to a linear–quadratic control problem with control constraints (saturated control). The numerical results give concrete hints for suitable jerk limitations in the setpoint generator of numerical control systems for machine tools, that otherwise has to be tuned heuristically. This will help to commission control systems for optimal machine performance based on the relevant mechanical system parameters.

References

1. Büskens C (1998) Optimierungsmethoden und Sensitivitätsanalyse für optimale Steuerprozesse mit Steuer- und Zustands-Beschränkungen, Dissertation, Institut für Numerische Mathematik, Universität Münster
2. Christiansen B., Maurer H., Zirn O. (2008) Optimal control of a voice-coil-motor with Coulombic friction, Proceedings 47th IEEE Conference on Decision and Control (CDC 2008), pp. 1557–1562, Cancun, Mexico
3. Fourer R., Gay D.M., Kernighan B.W. (2002) The AMPL Book, Duxbury Press, Brooks–Cole Publishing
4. Hartl R.F., Sethi S.P., Vickson R.G. (1995) A survey of the maximum principles for optimal control problems with state constraints, *SIAM Review*, 17, pp. 181–218.
5. Hermes H., LaSalle J.P. (1969) Functional analysis and time optimal control, *Mathematics in Science and Engineering*, 56, Academic Press, New York
6. Maurer H. (1977) On the minimum principle for optimal control problems with state constraints, *Schriftenreihe des Rechenzentrums der Universität Münster*, ISSN 0344-0842
7. Maurer H., Büskens C., Kim J.-H.R., Kaya C.Y. (2005) Optimization methods for the verification of second order sufficient conditions for bang–bang controls, *Optimal Control Applications and Methods*, 26, pp. 129–156
8. Maurer M., Osmolovskii N.P. (2004) Second order sufficient conditions for time-optimal bang-bang control problems, *SIAM J. Control and Optimization*, 42, pp. 2239–2263
9. Osmolovskii N.P., Maurer H. (2005) Equivalence of second order optimality conditions for bang–bang control problems. Part 1: Main results, *Control and Cybernetics*, 34, pp. 927–950; (2007) Part 2: Proofs, variational derivatives and representations, *Control and Cybernetics*, 36, pp. 5–45
10. Wächter A., Biegler L.T. (2006) On the implementation of a primal–dual interior point filter line search algorithm for large–scale nonlinear programming, *Mathematical Programming*, 106, pp. 25–57
11. Zirn O., Weikert S. (2006) *Modellbildung und Simulation hochdynamischer Fertigungssysteme*, Springer Verlag, Berlin
12. Zirn O.s (2007) *Machine Tool Analysis - Modelling, Simulation and Control of Machine Tool Manipulators*, Habilitation Thesis, Department of Mechanical and Process Engineering, ETH Zürich